Supplementary Information: "Generalized phase behavior of cluster formation in colloidal dispersions with competing interactions"

P. Douglas Godfrin,[a] Néstor Valadez-Pérez,[b] Ramon Castañeda-Priego,[b] Norman J. Wagner *[a] and Yun Liu,*[a,c]

[a] Department of Chemical and Biomolecular Engineering, University of Delaware, 150 Academy St, Newark, DE 19716 USA
[b] Division de Ciencias e Ingenieras, Universidad de Guanajuato, Loma del Bosque 103, 37150 Leon, Mexico.
[c] NIST Center for Neutron Science, National Institute of Standards and Technology, Gaithersburg, MD 20899.
*corresponding author e-mail: yun.liu@nist.gov (or yunliu@udel.edu), wagnernj@udel.edu

Each of the 8 HSDY and 5 LJY interaction potentials studied in the main text are plotted relative to each other in figure S1. The range of repulsion is constant among all potentials (fixed at 2σ) while the effective range of attraction varies from 1.0282σ to 1.4847σ and the relative strength of repulsion to attraction varies from 0.01 to 8. These parameters produce maximum repulsive interaction energy values ranging from 0.05k_BT to 3.0 k_BT and energy well depths ranging from -1.74 k_BT to -10.85 k_BT.

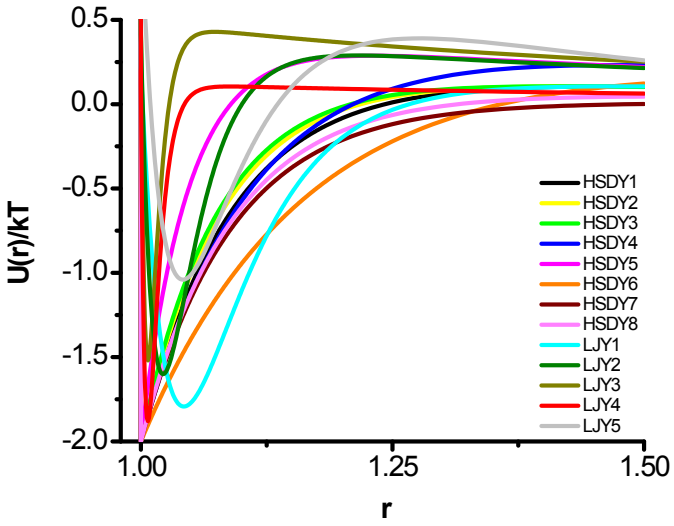

Figure S1

The critical behaviors of the reference attractive potentials (i.e., the attractive portion of the potentials in figure S1) are consistent with those reported for square well[1] and attractive Yukawa[2] fluids. The critical parameters of a representative square well potential (i.e., with the same B_{2c}^* value) of the reference attractive fluids are calculated. The critical reduced second virial coefficient of the reference attractive potential is calculated according to:

$$B_{2c}^* = \frac{B_2\left(T^* = T_c^*\right)}{B_2\left(T^* = \infty\right)} = 1 + 3\int_1^{r_c}\left(1 - exp\left(-\frac{U^{ref}(r,T_c^*)}{kT}\right)\right)r^2 dr \quad , \qquad (1)$$

which is used to calculate the effective range of attraction[1–3] of a square well fluid assuming the well depth is equal to $1/T_c^*$:

$$1+\delta=\left(1-\frac{1-B_{2c}^{*}}{1-\exp\left(\frac{1}{T_{c}^{*}}\right)}\right)^{1/3} \quad (2)$$

The trend in critical temperatures with the effective range of attraction is shown in figure S2 and follow the expected trends.[1,2] Deviations are expected for ranges ~ 1.1 as the ELCS becomes invalid.[3] The HSDY potential is normalized such that the well depth is always equal to $1/T_c^*$ while the LJY potential is not. Therefore, the effective range of attraction for LJY potentials depends on the definition of the well depth, which is described in more detail below.

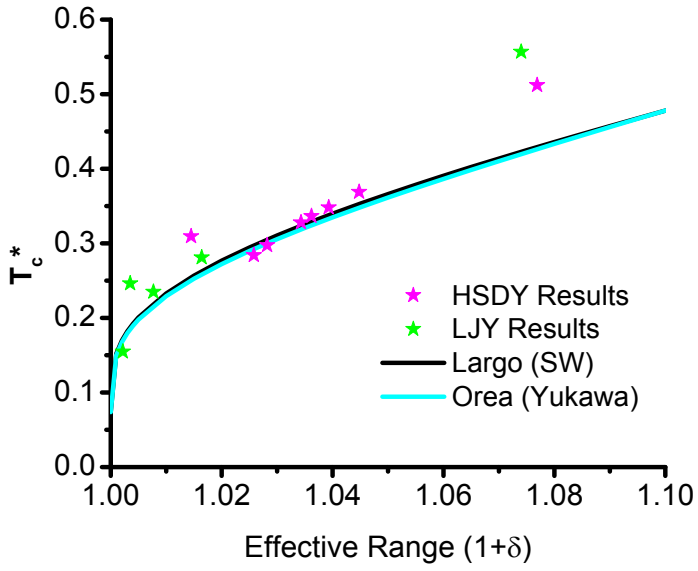

Figure S2

Calculating the effective range of attraction of an LJY potential is sensitive to the well depth defined in the corresponding square well potential. Figure S3a demonstrates the effect of defining the well depth as $1/T_c^*$ (T_c^*) or as the minimum in the potential at T_c^* (U_{min}) as shown by green and red stars, respectively. T* values calculated previously are given for a square well potential[1] (black line) and an attractive Yukawa potential[2] (cyan line). The effective square well potentials used to calculate the effective range of attraction of the circled stars in figure S3a are plotted relative to each other in figure S3b.

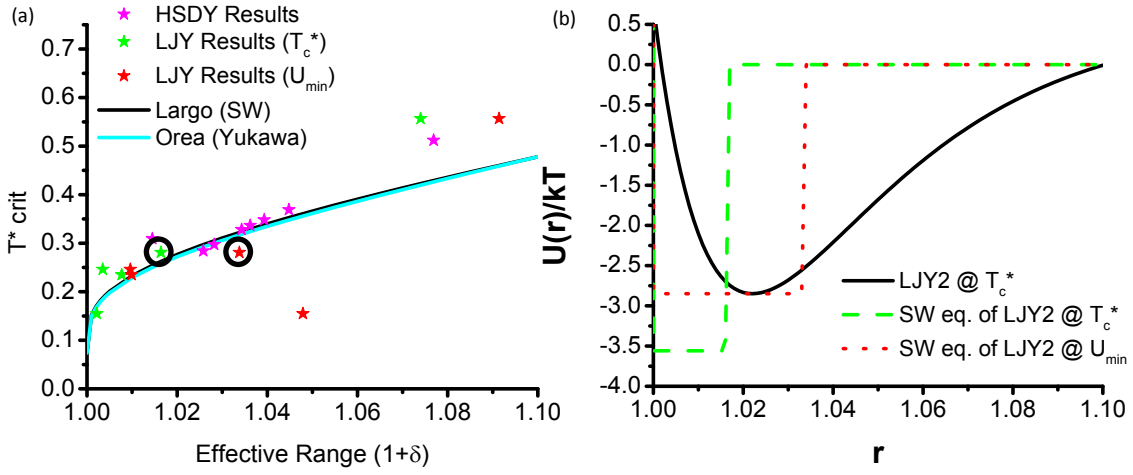

Figure S3

In figure S4, the tau parameters, τ, where $B_2^* = 1-1/4\tau$, at the critical point for the potentials used here are compared to the expected value according to the Noro-Frenkel ELCS[3] as a function of the calculated effective range of attraction. The three circled points correspond to the three potentials discussed in the main text as having the shortest ranges of attraction. These points have the largest deviations from the ELCS expectations, most likely due to inaccuracies of the DPT method used to estimate T_c^* under these conditions. The large deviations from ELCS expectations at larger effective ranges of attraction are likely due to the proximity to the upper range of validity of ELCS.

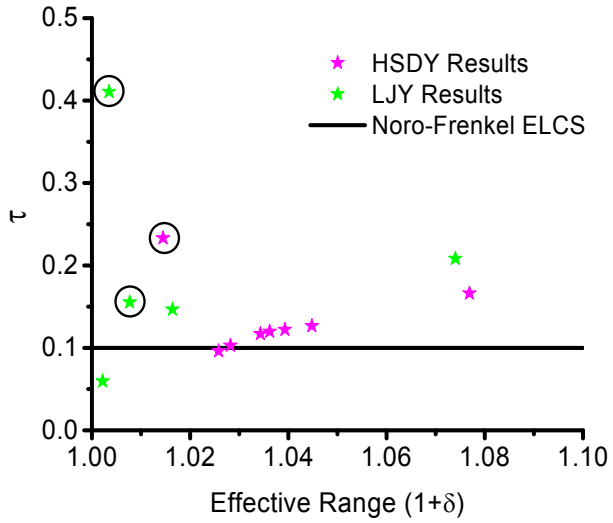

Figure S4

The configuration energy per particle of a single cluster as a function of cluster size, plotted in figure S5, is reproduced from the previous work by Sciortino et. al.,[4] shown as the lines for four different sets of interaction parameters for a potential that combines a Yukawa repulsion term and a Leonard-Jones α-2α attraction term. That work used a modified basin-hopping algorithm in Monte Carlo (MC) simulations to calculate the minimum energy structure for each cluster size. The data points are those calculated in this work by assuming a spherical FCC cluster structure, which nearly exactly reproduce the results found by the more elaborate MC method.

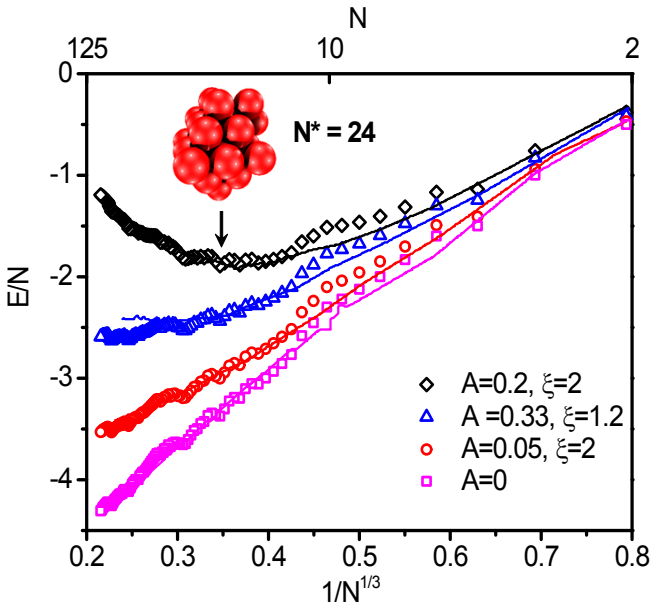

Figure S5

In figure S6a below, the necessary value of z_1 is shown, along with the corresponding value of maximum interaction energy, E_{max}, as a function of z_2 that maintains consistent values of B_{2c}^* and r_c as z_2 is varied for a state point (φ = 0.05, T* = 0.25) from potential HSDY1 (see Table 1). The transition from clustered states to dispersed fluids by the same state point as a function of z_2 is shown to coincide with a numerical model of cluster stability in figure S6b. The simulation points are plotted on the line of λ as a function of z_2 also needed to maintain B_{2c}^* and r_c values. The numerical model consists of single spherical clusters of face centered, body centered, and simple cubic models (FCC, BCC, SC, respectively). As shown in figure S5, conditions conducive to cluster formation are determined by a minimum in the configuration energy as a function of cluster size. With large enough strength and range of repulsion (large λ and small z_2, respectively) the balance of attraction and repulsion is sufficient to stabilize finite sized clusters. The transition from clustered states to dispersed fluid states corresponds with a packing fraction model between the BCC and DC lattices, similar to that found in figure 7 of the main text.

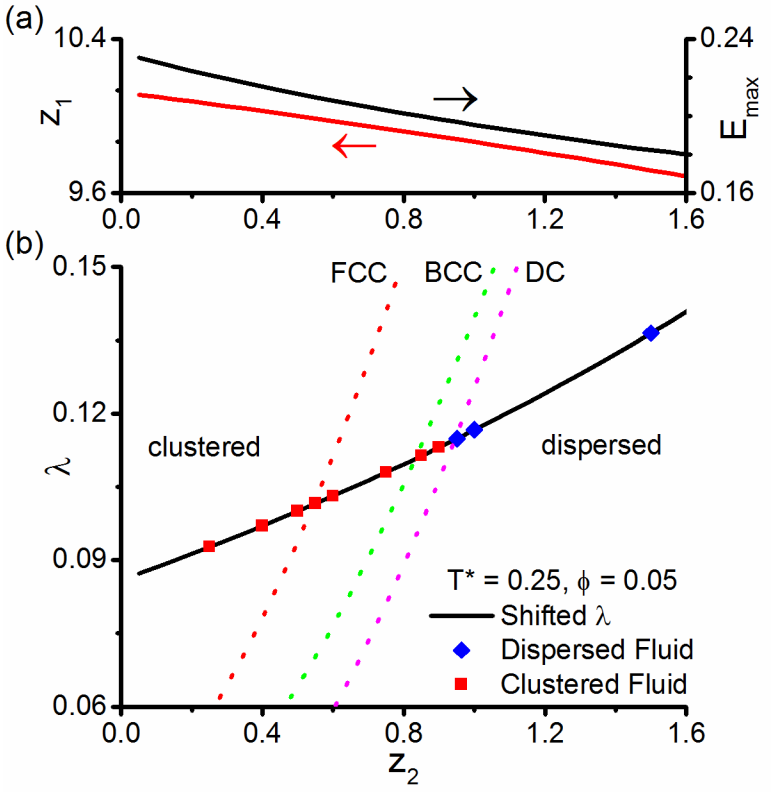

Figure S6

The effect of changing the range of repulsion while maintaining constant values of the B_2* for the reference attractive potential and r_c is shown below in figure S7 (for T* = 0.25). The attractive portion of all potentials overlap while the inset demonstrates the maximum interaction energy becomes smaller as the range becomes smaller. Above a z_2 of about 0.8, repulsion is not significant enough to produce stable clusters according to the simple ground state model described in the main text.

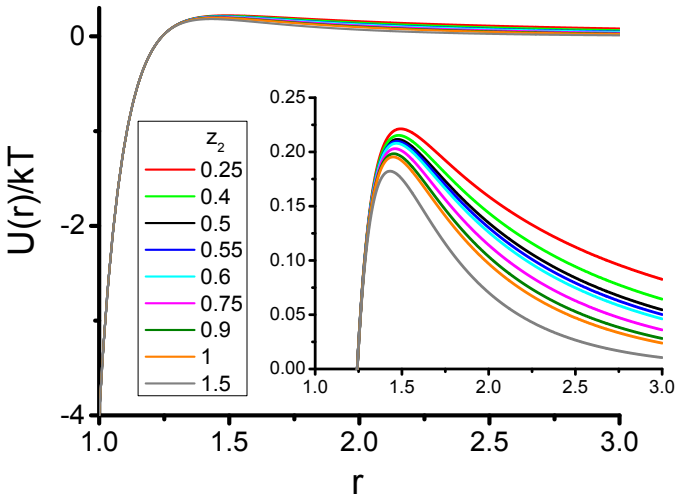

Figure S7

Structure factors are calculated for each of the potentials shown in figure S7 at the state point $\phi = 0.05$, $T^* = 0.25$. Each of the states produces an IRO peak even though above a z_2 of roughly 0.8 the states transition from clustered to dispersed fluids. This transition is shown to correspond with a drop in the magnitude of the IRO peak below a value of about 2.7, as shown below in figure S8a, which is a proposed empirical rule for distinguishing clustered states. The dispersed fluid states at $z_2 = 1.5$ are above this limit; however, the peak position has shifted to smaller q-values and the magnitude of S(q=0) has increased, suggesting a shift towards an attraction dominated microstructure approaching phase separation. The proposed limit of an average coordination number of 2.4 or greater for clustered states also appears to be applicable for these same states with varying range of repulsion, shown in figure S8b.

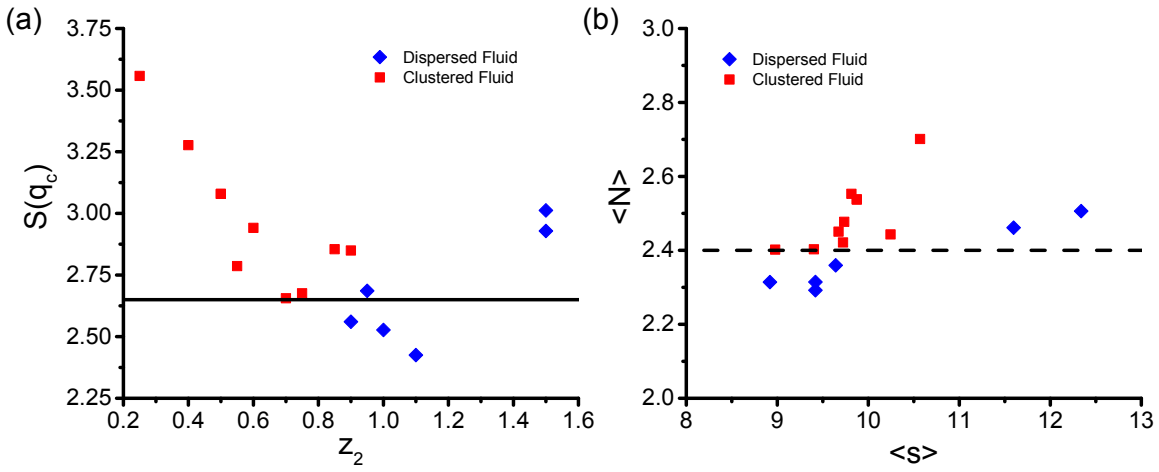

Figure S8

References

1. J. Largo, M. A. Miller, and F. Sciortino, *J. Chem. Phys.*, 2008, **128**, 134513.
2. P. Orea, C. Tapia-Medina, D. Pini, and A. Reiner, *J. Chem. Phys.*, 2010, **132**, 114108.
3. M. G. Noro and D. Frenkel, *J. Chem. Phys.*, 2000, **113**, 2941.
4. F. Sciortino, S. Mossa, E. Zaccarelli, and P. Tartaglia, *Phys. Rev. Lett.*, 2004, **93**, 5.